THE JOURNAL OF PHYSICAL CHEMISTRY C

Article

pubs.acs.org/JPCC

Impact of Molecular Charge-Transfer States on Photocurrent Generation in Solid State Dye-Sensitized Solar Cells Employing Low-Band-Gap Dyes

Sai Santosh Kumar Raavi,[†,∥,⊥] Pablo Docampo,[‡,⊥] Christian Wehrenfennig,[‡] Marcelo J. P. Alcocer,[†,§] Golnaz Sadoughi,[‡] Laura M. Herz,[‡] Henry J. Snaith,*[,‡] and Annamaria Petrozza*[,†]

[†]Center for Nano Science and Technology @PoliMi, Istituto Italiano di Tecnologia, Via Pascoli 70/3, 20133 Milano, Italy

[‡]Clarendon Laboratory, Department of Physics, University of Oxford, Parks Road, Oxford OX1 3PU, United Kingdom

[§]Dipartimento di Fisica, Politecnico di Milano, Piazza Leonardo da Vinci 32, 20133 Milano, Italy

Supporting Information

ABSTRACT: "Push−pull" structures have been considered a winning strategy for the design of fully organic molecules as sensitizers in dye-sensitized solar cells (DSSC). In this work we show that the presence of a molecular excited state with a strong charge-transfer character may be critical for charge generation when the total energy of the photoexcitation is too low to intercept accepting states in the TiO_2 photoanode. Though hole transfer to the 2,2′,7,7′-tetrakis(*N*,*N*-di-*p*-methoxyphenylamine)-9,9′-spirobifluorene can be very fast, an electron−hole pair is likely to form at the organic interface, resulting in a possible traplike excitation. This leads to poor photocurrent generation in the solid state DSSC (ss-DSSC) device. We demonstrate that it is possible to overcome this issue by fabricating SnO_2-based ss-DSSC. The resulting solar cell shows, for the first time, that a SnO_2-based ss-DSSC can outperform a TiO_2-based one when a perylene-based, low-band-gap, push−pull dye is used as sensitizer.

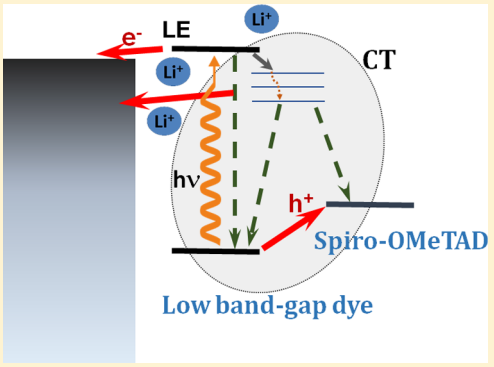

INTRODUCTION

In the field of excitonic solar cells, fully organic bulk-heterojunction solar cells and dye-sensitized solar cells (DSSC) have represented the two main research avenues in the past 20 years. Solid state dye-sensitized solar cells, first proposed by Bach and co-workers in 1998,[1] can be considered a proper "hybridization" between the former categories. They replaced the I^-/I_3^- redox electrolyte with an organic semiconductor, 2,2′-7,7′-tetrakis(*N*,*N*-di-*p*-methoxyphenylamine)-9,9′-spirobifluorene (Spiro-OMeTAD) as hole transporter material (HTM), to regenerate the photooxidized dye and transport charges. The first reported solid state DSSC (ss-DSSC) used a 4.2 μm thick mesoporous TiO_2 film, sensitized with a low-extinction-coefficient dye (N719). It exhibited a power conversion efficiency below 1%, while the same dye already showed an efficiency of over 7% when employed with a redox electrolyte.[2]

Solid state DSSCs had a slow take off, but their development sped up significantly after a power conversion efficiency (PCE) of 5% was demonstrated, establishing it as a serious contender in the field of low-cost photovoltaics. By substituting the I^-/I_3^- redox couple with a one-step dye regeneration process material, higher power conversion efficiencies can be targeted,[3] as the associated loss in potential is reduced. However, this substitution brings about a strong reduction of the dielectric constant at the photoactive interface, negatively impacting charge separation and inducing greater recombination losses between holes in the hole transporter and electrons in the mesoporous structure.[4] For this reason, ss-DSSCs suffer from severe thickness constraints,[5,6] with maximum PCEs achieved for 2−3 um thick films. These are however not thick enough to absorb all available solar irradiation under conventional Ruthenium-based sensitization. This leads to the necessity of improving the light harvesting capability of the dye, moving the attention to fully organic dye molecules which generally show much higher extinction coefficients than their ruthenium-based counterparts.[7] Lots of activities have been focused on the use of push−pull organic dyes, consisting of molecules with strong electron donating and accepting moieties, which should sustain the formation of excited states with a strong charge-transfer character.[7,8]

In past years, perylene-based dyes have attracted much attention, offering the possibility of strongly tuning the intramolecular charge transfer (ICT) of the intrachain photoexcitation together with the tuning of the absorption spectrum. When these dyes are employed in electrolyte-based DSSCs,

Special Issue: Michael Grätzel Festschrift

Received: January 3, 2014
Revised: May 16, 2014
Published: May 16, 2014

   dx.doi.org/10.1021/jp5000667 | *J. Phys. Chem. C* 2014, 118, 16825−16830

Edvinsson et al. demonstrated that the devices showed better performance when the strength of the molecular ICT was enhanced. This was attributed to an improvement in charge generation.[9] However, they also found a threshold in the ICT strength, above which no further gains are achieved in electrolyte-based devices, while it is still performing well for charge generation in ss-DSSC.[10,11] Fast reductive quenching, where hole transfer from the dye to the HTM happens before electrons have a chance to transfer into the mesoporous metal oxide, has been considered a possible mechanism favoring charge generation in ss-DSSC.[23] In fact, it may be beneficial when, with the intent of reducing the sensitized band gap for solar spectrum matching and for reducing the loss in potential, the energy gap between the lowest unoccupied molecular orbital (LUMO) level of the dye and the effective conduction band (CB) edge of TiO_2 is minimized. In fact, the latter would slow down the electron-transfer rate.[12] While on the other hand, once hole transfer is complete, free electrons on the dye can be more easily transferred to the metal oxide. However, this assumes that the hole in the hole conductor and the electron on the dye are already fully uncorrelated.

In this work we show that the presence of a molecular excited state with a strong charge-transfer character may be critical for charge generation when the total energy of the photoexcitation is too low to intercept accepting states in the TiO_2 photoanode. Though hole transfer to the Spiro-OMeTAD can be very fast, an electron−hole pair is likely to form at the organic interface, resulting in a possible traplike state. This leads to poor photocurrent generation in the ss-DSSC device. However, when mesoporous TiO_2 is replaced by SnO_2, the CB of which is about 0.3−0.5 eV farther from the vacuum level than in TiO_2, the photocurrent of the resulting cell doubles leading—for the first time—to higher power conversion efficiency compared to the corresponding TiO_2-based cell.

METHODS

Sample Preparation. Fluorine-doped tin oxide (FTO) coated glass sheets (15 Ω/□, Pilkington) were etched with zinc powder and HCl (4 M) to obtain the required electrode pattern. The sheets were then washed with soap (2% Hellmanex in water), deionized water, acetone, and ethanol and finally treated under an oxygen plasma for 10 min to remove the last traces of organic residues. The FTO sheets were subsequently coated with a nonporous layer of either SnO_2 (100 nm) for SnO_2-based devices or TiO_2 for titania-based devices. This layer was deposited by aerosol spray pyrolysis of the appropriate precursor (95% butyltin trichloride (Sigma-Aldrich) or titanium diisopropoxide bis-(acetylacetonate)) mixed with ethanol in a 1:10 precursor:-ethanol ratio at 450 °C using air as the carrier gas. During the deposition of the compact layer, the electrodes were masked so that the metal oxide layer only covered the FTO and not the etched glass (otherwise short-circuiting would occur). A homemade SnO_2 mesoporous paste was prepared in a way similar to that used by Ito et al. and as published previously,[21,22] from <100 nm particle size nanopowder (549657 Sigma-Aldrich) for tin-oxide-based photoanodes while Dyesol NR18-T paste was used for titania-based photoanodes.

The mesoporous layers were prepared via doctor blading by hand using Scotch tape and a pipet on the appropriate nonporous metal-oxide-coated FTO substrates to achieve a final thickness of 1.5−2 μm. The substrates were then slowly heated to 500 °C (ramped over 1.5 h) and baked at this temperature for 30 min in air. After cooling, slides were cut down to size and soaked in either 20 mM magnesium acetate (SigmaAldrich) in ethanol bath for 1 min on a hot plate set at 100 °C (boiling the ethanol in the bath) for tin-oxide-based devices or in a 20 mM aqueous $TiCl_4$ solution at 70 °C for 1 h for titania-based photoanodes. After rinsing with ethanol and drying in air, the tin oxide photoanodes were coated with a paste of Al_2O_3 nanoparticles, as detailed previously,[22] to give a buffer layer with a dry film thickness of 100 nm to prevent shunting paths, while no further processing was performed on titania-based photoanodes. The substrates were subsequently baked once more at 500 °C for 45 min in air, then cooled to 70 °C, and finally immersed in a dye solution for 1 h. The perylene-based dye termed ID504 was dissolved in a 0.2 mM concentration in dichloromethane. Spiro-OMeTAD was dissolved in chlorobenzene at 15 vol % concentration, and after the hole transporter was fully dissolved, 4-*tert*-butylpyridine (*t*BP) was added with a volume to mass ratio of 1:26 (μL mg^{-1}) tBP:spiro-OMeTAD. Lithium bis(trifluoromethylsulfonyl)imide salt (Li-TFSI) was predissolved in acetonitrile at 170 mg mL^{-1} and added to the hole transporter solution at 1:12 (μL mg^{-1}) Li-TFSI solution:Spiro-OMeTAD. The dyed films were rinsed briefly in dichloromethane and dried in air for 1 min.

Immediately after drying, a small quantity of the hole transporter solution (22 μL) was dispensed onto each substrate and was then spin-coated at 1500 rpm for 40 s in air. After spin-coating the hole transporter, the films were left overnight in an air atmosphere in the dark before they were placed in a thermal evaporator where 150 nm thick silver electrodes were deposited through a shadow mask under high vacuum (10^{-6} mbar). To measure the photovoltaic properties correctly, the active areas of the devices were defined by metal optical masks with 0.09−0.125 cm^2 apertures that were glued onto the illuminated side. The typical photoelectrode area as defined by the overlap between the silver electrode and the FTO was around 0.15 cm^2. Spectroscopy samples were prepared in the same way, but the FTO substrate was replaced with either a quartz substrate for terahertz (THz) measurements or a microscope glass slide for all other substrates. In order to deposit the additives without the hole transporter, the same amount of tBP and Li-TFSI was added to chlorobenzene and this solution was then spin-coated following the same protocol as for the spiro-containing devices.

Time-Resolved Photoluminescence. Time-resolved photoluminescence (PL) measurements were performed using a femtosecond laser source and streak camera detection system. An unamplified Ti:Saphire laser (Coherent Chameleon Ultra II) operating at 80 MHz was tuned to provide pulses with central wavelengths of 980 nm, energies of ∼10 nJ, and temporal and spectral bandwidths of ∼140 fs and ∼5 nm, respectively. A β-barium borate crystal provided type I phase-matched second harmonic generation, leading to pulses with central wavelengths of 490 nm. These were focused onto the sample, maintaining a low fluence (<30 mJ/cm^2, ∼100 um spot diameter) in order to avoid any saturation effects in the sample. The resulting collected emission was analyzed by a spectrograph (Princeton Instruments Acton SP2300) coupled to a streak camera (Hamamatsu C5680) equipped with a synchroscan voltage sweep module. In this way, measurements of photoluminescence intensity as a function of both wavelength and time were obtained with spectral and temporal resolutions of ∼1 nm and ∼3 ps, respectively. Temporal broadening of the pump pulses caused by dispersive elements

dx.doi.org/10.1021/jp5000667 | J. Phys. Chem. C 2014, 118, 16825−16830

was confirmed to be well below the response time of the detection system.

Optical−Pump−THz−Probe Spectrocopy. The optical−pump−THz−probe setup[18] uses a Ti:Saphire regenerative amplifier to generate 40 fs pulses at 800 nm wavelength and a repetition rate of 1.1 kHz. Terahertz pulses are generated by optical rectification in a 2 mm ZnTe or a 450 μm thick GaP crystal and detected by electrooptic sampling in another ZnTe crystal of 0.2 mm thickness. Samples are optically excitated at 545 nm wavelength using the output of an optical parametric amplifier (OPA). Measurements have been performed with the THz beam path and the sample in an evacuated chamber, at a pressure of about 10^{-1} mbar.

RESULTS AND DISCUSSION

Figure 1a shows the chemical structure of the perylene-based dye termed ID504, which has a strong push−pull character; i.e.,

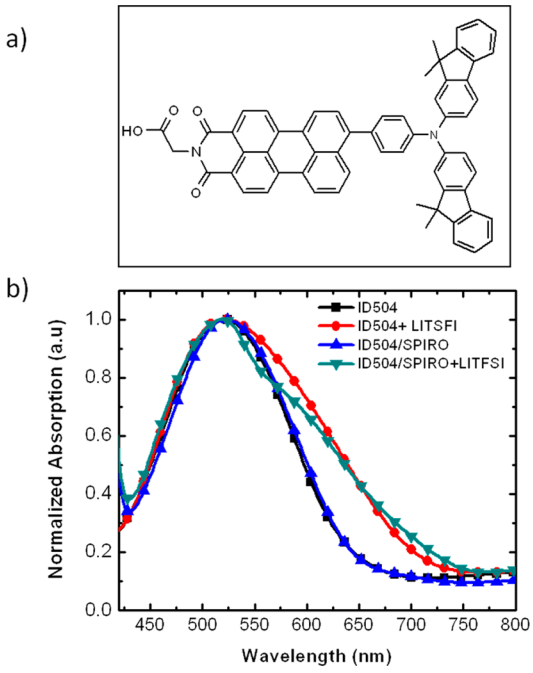

Figure 1. (a) Chemical structure of the perylene-based dye termed ID504; (b) ID504 absorption spectra when adsorbed on an Al_2O_3 mesoporous substrate (squares), and in different environments: with Li-TFSI salts (circles), pristine Spiro-OMeTAD (up triangles), and Li-TFSI-salts-doped Spiro-OMeTAD (down triangles).

the highest occupied molecular orbital (HOMO) lies mainly on the triarylamine unit and the lowest unoccupied molecular orbital (LUMO) is strongly localized on the perylene unit. Figure 1b shows the dye absorption spectra when adsorbed on an insulating Al_2O_3 mesoporous substrate (which allows retention of the same morphology expected in standard DSSC photoanodes) in different environments. No change is observed when pristine Spiro-OMeTAD is deposited on the dye, while the Li-TFSI salts—commonly used as an additive to improve the photovoltaic performance of ss-DSSCs[12,13]—induce a strong broadening of the spectrum at longer wavelengths. The broadening is further resolved into a shoulder when the dye is interfaced to the hole conductor doped with the Li-TFSI.

Figure 2 shows the time-resolved photoluminescence spectra of the same samples, at 4 ps and 1 ns after photoexcitation at

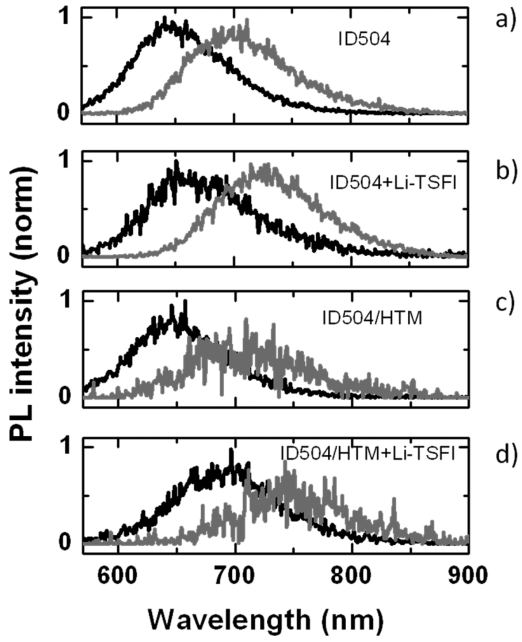

Figure 2. Time-resolved photoluminescence spectra gated at 4 ps (black) and 1 ns (gray) upon photoexcitation for ID504 adsorbed on an Al_2O_3 mesoporous substrate (a) and in different environments: (b) with Li-TFSI salts, (c) pristine Spiro-OMeTAD, and (d) Li-TFSI-salts-doped Spiro-OMeTAD. Excitation was at 490 nm; fluence was at 10^{13} photons/cm^2. Samples were measured in a vacuum chamber (10^{-6} mbar).

490 nm. The Al_2O_3/ID504 sample, at 4 ps, shows a broad spectrum peaking at 645 nm which shifts to 700 nm in the first nanosecond (Figure 2a). Similar behavior is observed for Al_2O_3/ID504/Spiro-OMeTAD (Figure 2c). The scenario changes when the Li-TFSI salts are added. At 4 ps, the spectrum of Al_2O_3/ID504 with Li-TFSI still peaks at 645 nm at early times but shifts to 725 nm within the first 1 ns (Figure 2b). Further changes are observed when Li-TFSI-doped hole transporter is deposited on the dye. At 4 ps the PL spectrum already peaks at 700 nm, with a shoulder at 660 nm, before shifting to 745 nm in the first nanosecond (Figure 2d). We rationalize these results based on the presence of a molecular intrachain charge-transfer state. Due to its dipolar character, this state is extremely sensitive to the molecular environment, in particular, to the medium dielectric and local electric fields. Experimental results on conjugated push−pull molecules suggest that in the case of a Marcus-type nonadiabatic electron-transfer process, these systems exhibit a locally excited localized singlet state and the CT state, whose equilibrium energy and oscillator strength depend on the medium-induced stabilization of the CT state and the temperature of the system.[8,14] Depending on the strength of the electron donor/acceptor moieties of the molecules and on the strength of the dielectric/local electric field in the molecular environment, the intrachain CT can also be observable as a ground state absorption feature as demonstrated in Figure 1.

Time-resolved PL spectroscopy reveals that when exciting at 490 nm, the primary localized molecular exciton is first generated and, then, intrachain charge transfer occurs. When Li-TFSI salts are introduced, the primary excitation lifetime shortens and a more red-shifted CT emission peak with a longer lifetime emerges. This is the result of ionic charges, which have the potential to stabilize CT states in conjugated

dx.doi.org/10.1021/jp5000667 | J. Phys. Chem. C 2014, 118, 16825−16830

molecules by establishing local Coulomb fields that perturb the HOMO and LUMO orbital energies.[13,15] The distribution of both anions and cations around the dye monolayer is thus expected to lead to local configurations where electron−hole pairs are separated under the influence of ions but the resulting state has also a lower total energy with respect to the vacuum level.

It is interesting to note here that when the ID504 is interfaced with the Li-TFSI-doped Spiro-OMetad, the emission shows a further red shift. It must be noted that the density of ions around the dye is expected to be lower. In fact the samples without and with the hole transporter were prepared using the same additive concentration; thus, in the presence of the HTM the ions will be dispersed also within the hole transporter molecular film.. This seems to suggest that salts are not only stabilizing the dye intramolecular CT state but also inducing the formation of an emissive intermolecular CT state at the interface between the dye and the Spiro-OMeTAD molecule. Femtosecond-transient absorption (fs-TA) experiments show that hole transfer from the dye to the spiro starts in the sub-picosecond time regime and is completed in tens of picosecond (see Figure S1 in the Supporting Information (SI)). However, we can infer from the photoluminescence data that this does not lead to 100% yield of free charges but to correlated electron−hole pairs which are eventually radiatively coupled to the ground state. The high-band-gap Al_2O_3 prevents electron transfer into its CB, and thus a different behavior may be expected when this material is integrated in the photovoltaic devices.

In order to shed light on the role of interfacial states in the complete devices, further investigations have been performed on TiO_2/ID504/HTM samples. In this configuration, upon photoexcitation, the intrachain electron transfer which stabilizes the photoexcitation in a CT state at lower energy with respect to the vacuum level is in competition with electron transfer at the dye/oxide interface from the localized molecular excitation. If hole transfer to the Spiro-OMeTAD is quicker than electron transfer to the metal oxide, reductive quenching of the photoexcitation can be observed. The fs-TA spectra are unfortunately quite congested, and only qualitative information can be extracted. The primary excitation is only partially quenched, and the intrachain electron transfer which leads to the stabilization of the CT state in the presence of the Al_2O_3 electron blocking layer is in competition with electron transfer to the TiO_2 (see Figure S2 in the SI). Hole transfer still starts in the sub-picosecond time regime (see Figures S2 and S3 in the SI); however, it becomes more difficult to probe in the presence of Li-TSFI as electroabsorption-like features[11,16] and/or the photoinduced absorption (PA) band of the singlet CT state further stabilized overlap with the hole PA band (see Figure S4 in the SI).

THz time-resolved spectroscopy is a highly useful tool for investigating the dynamics of free charge carriers. In an optical−pump−terahertz−probe (OPTP) experiment, the sample is excited by an optical pulse and, then, after a well-defined delay, the sample is probed by a terahertz pulse, which is mainly sensitive to the presence of free charges. This allows studying dynamics of charge injection, trapping, and recombination with picosecond resolution. In particular, it avoids the complex process of band assignment necessary in optical probe transient absorption spectroscopy. Figure 3a shows the THz-photoinduced absorption, which is proportional to free carriers conductivity (i.e., the product of mobility and charge density),

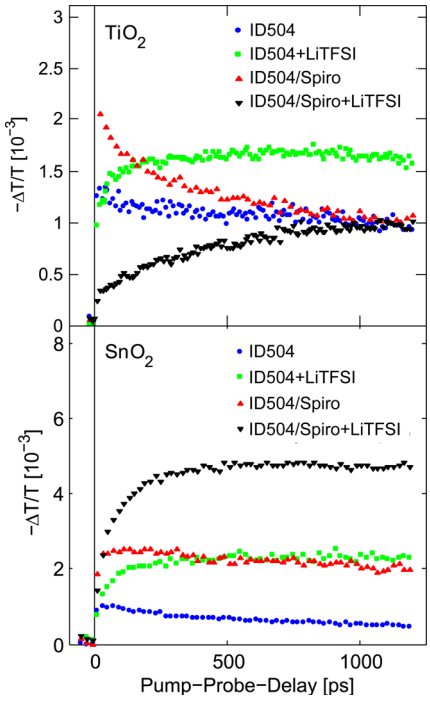

Figure 3. THz-photoconductivity dynamics in nanoporous (a) TiO_2 and (b) SnO_2 films sensitized with ID504 dye in different environments, i.e., with Li-TFSI salts, pristine Spiro-OMeTAD, and Li-TFSI-salts-doped Spiro-OMeTAD. Excitation was at 545 nm; incident photoexcitation fluence was ~5 × 10^{13} photons/cm^2.

for the dye-sensitized TiO_2 nanoporous films as a function of time after excitation of ID504 dye at 545 nm. The metal oxide material has a sufficiently large band gap allowing almost exclusive excitation of the dye sensitizer. In this way, the measured photoconductivity signal originates from mobile electrons subsequently injected into the metal oxide films, while the holes on the dye molecules are essentially stationary. TiO_2/ID504 and TiO_2/ID504/HTM samples show that within the time resolution of the experiment of about 1 ps, electron injection is already complete. The subsequent decay dynamic can either be related to charge recombination or to a trapping of the mobile electrons in trap states available in the inorganic semiconductor. More intriguing are the dynamics in the presence of Li-TFSI. Notably, Li^+ ions influence the position of the TiO_2 conduction band, inducing larger absolute values once adsorbed on the metal oxide surface. In principle this should induce a faster rate of electron injection into the semiconductor, due to a larger energy gap between the primary photoexcitation and the TiO_2 accepting states[11,12] Despite this, OPTP reveals a slowing of the injection process in the presence of Li^+, a phenomenon which becomes even more important when the HTM is present (growth of the photoconductivity up to 1.2 ns). Interestingly, the injection dynamics become slower as the CT states identified by time-resolved PL are stabilized and their total energy is reduced (see SI for a quantitative analysis of the PL and OPTP dynamics, correlating the two experiments) . The slower kinetics observed in the presence of the HTM seem also to corroborate our previous hypothesis regarding the formation of an interfacial state at the organic interface. These interfacial states in principle can act as intermediate states for charge separation. However, in this context they would result in undesired trap states, preventing the reductive quenching of the primary photoexcitation and

dx.doi.org/10.1021/jp5000667 | J. Phys. Chem. C 2014, 118, 16825−16830

reducing the photocurrent generation probability due to their radiative coupling to the ground state. Furthermore, a weaker driving force for charge injection at the interface results in higher potential losses, thus raising an ubiquitous problem when moving to lower-band-gap dyes or push−pull systems where the relaxed CT states are stabilized at lower energies with respect to the primary photoexcitation.

We have also tested the same dye on SnO_2-based mesoporous photoanodes. SnO_2 exhibits a bulk mobility almost 2 orders of magnitude higher than that of TiO_2, and its CB edge is 350−500 mV more positive than that of TiO_2.[17] This implies that SnO_2 should be more suitable for use with very narrow band gap sensitizers. However, to date, TiO_2-based devices have always resulted in higher photovoltaic performance.

Figure 3b shows the photoconductivity dynamics of a complete set of samples which include SnO_2/ID504 and SnO_2/ID504/HTM with and without Li-TFSI. Charge injection in sensitized SnO_2 takes place within tens of picoseconds (generally on a time scale slower than that observed for TiO_2, independently of the dye used[17,18]). Then, a slight decay starts, which is recovered in the presence of Spiro-OMeTAD. Notably, when these samples are doped by Li-TFSI, though the electron injection time slows due to the stabilization of the CT state, the dynamics is completed in 300 ps without Spiro-OMeTAD and in 600 ps with Spiro-OMeTAD. This suggests that large absolute values of the CB edge of the metal oxide aids collection of charges from low-energy excitonic species.

Finally, we have tested the dye in a working ss-DSSC device employing the two different metal oxides. Figure 4 shows the current−voltage curves and the external quantum efficiency (EQE) spectra for ss-DSSCs based on TiO_2 and SnO_2 photoanodes. The SnO_2 surface has been modified by an extremely thin MgO passivation layer, which notably slows the electron injection at the interface (see Figure S7 in the SI for OPTP investigation of these photoanodes) while reducing the charge recombination losses at the hybrid interface.[19,20] We observe that the short-circuit current is more than doubled in the SnO_2-based device (8.4 mA cm^{-1} with respect to 4 mA; see Figure 4) with an EQE peak of 80% (Figure 4b). This leads to a power conversion efficiency of the device of about 3%, overtaking, for the first time, the equivalent TiO_2-based device which shows less than 2% power conversion efficiency.

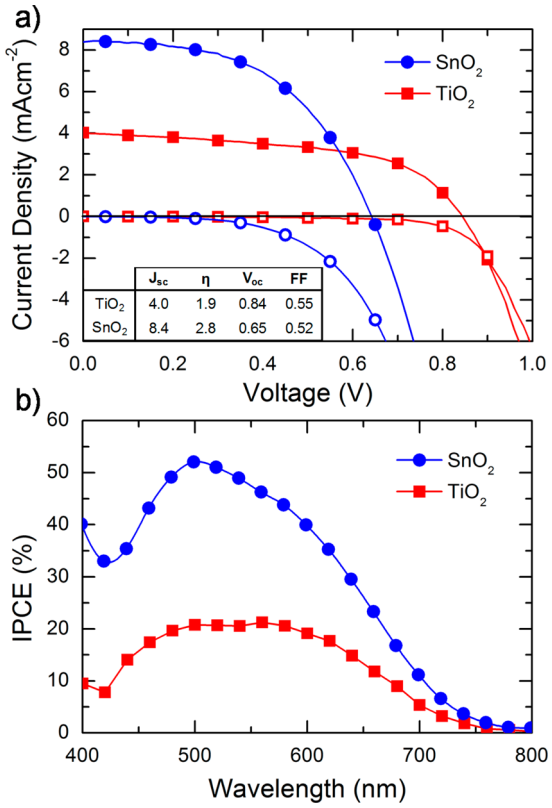

Figure 4. (a) Current/voltage characteristics under simulated solar conditions measured for ss-DSSC fabricated from either TiO_2 or SnO_2 nanoporous films sensitized with ID504 dye. As inset, the table reports the main figures of merit of the photovoltaic devices. (b) Photovolatic action spectra for TiO_2- and SnO_2-based DSSC incorporating ID504 as the sensitizer.

CONCLUSION

In conclusion, we show that the "push−pull" paradigm considered so far for the molecular design of fully organic molecules must be carefully handled. Efficient design of the hybrid interface in the presence of low-band-gap dyes is a critical issue. This is mainly due to the compromise between good solar spectrum match, good open-circuit voltage, and good energy level alignment at the hybrid interface which will influence the electron/hole transfer rate. Most of the time, the lowest excited state of the dye is very close to the semiconductor conduction band (if not resonant with trap states), thus making the electron-transfer process very inefficient and reductive quenching a strategic solution. We find that when the molecular exciton is stabilized in a low-energy CT state through efficient intramolecular electron transfer, if the metal oxide presents a significant energy barrier, the photoexcited state may remain trapped at the organic interface, though hole transfer from the dye to the HTM happens efficiently. This will lead to a loss in charge generation. Thus, a material shift paradigm must be considered in order to make the most of low-band-gap dyes. Here we implemented this strategy employing SnO_2 as an alternative to the dominating TiO_2 as photoanode material. This yields, overall, more efficient devices due to higher short-circuit currents, demonstrating, for the first time, a dye which performs better in a SnO_2 than a TiO_2-based solid state DSSC.

ASSOCIATED CONTENT

Supporting Information

Figures showing fs-transient absorption spectra, THz and PL dynamics fitting, and THz spectra from MgO passivated SnO_2 photoanodes and text describing the transient absorption methods used. This material is available free of charge via the Internet at http://pubs.acs.org.

AUTHOR INFORMATION

Corresponding Authors

*(A.P.) E-mail: annamaria.petrozza@iit.it.
*(H.J.S.) E-mail: h.snaith1@physics.ox.ac.uk.

Present Address

[‖]Division of Physics and Applied Physics, School of Physical and Mathematical Sciences, Nanyang Technological University, 21 Nanyang Link, Singapore 637371.

Author Contributions

[⊥]S.S.K.R. and P.D. contributed equally to this work.

Notes

The authors declare no competing financial interest.

■ ACKNOWLEDGMENTS

This work was financially supported by the European Union Seventh Framework Programme [FP7/2007-2013] under Grant Agreement 316494.

■ REFERENCES

(1) Bach, U.; Lupo, U.; Comte, P.; Moser, J. E.; Weissoertel, F.; Salbeck, J.; Spreitzer, H.; Grätzel, M. Solid-State Dye-Sensitized Mesoporous TiO_2 Solar Cells with High Photon-to-Electron Conversion Efficiencies. *Nature* **1998**, *395*, 583−585.

(2) Nazeeruddin, M. K.; Kay, A.; Rodicio, I.; Humphry-Baker, R.; Müller, E.; Liska, P.; Vlachopoulos, N.; Grätzel, M. Conversion of Light to Electricity by cis-X_2Bis(2,2′-bipyridyl-4,4′-dicarboxylate)-ruthenium(II) Charge-Transfer Sensitizers (X = Cl^-, Br^-, I^-, CN^-, and SCN^-) on Nanocrystalline TiO_2 Electrodes. *J. Am. Chem. Soc.* **1993**, *115*, 6382−6390.

(3) Snaith, H. J. Estimating the Maximum Attainable Efficiency in Dye-Sensitized Solar Cells. *Adv. Funct. Mater.* **2010**, *20*, 13−19.

(4) Snaith, H. J.; Schmidt-Mende, L. Advances in Liquid-Electrolyte and Solid-State Dye-Sensitized Solar Cells. *Adv. Mater.* **2007**, *19*, 3187−3200.

(5) Docampo, P.; Hey, A.; Guldin, S.; Gunning, R.; Steiner, U.; Snaith, H. J. Pore Filling of Spiro-OMeTAD in Solid-State Dye-Sensitized Solar Cells Determined via Optical Reflectometry. *Adv. Funct. Mater.* **2012**, *22*, 5010−5019.

(6) Docampo, P.; Guldin, S.; Steiner, U.; Snaith, H. J. Charge Transport Limitations in Self-Assembled TiO_2 Photoanodes for Dye-Sensitized Solar Cells. *J. Phys. Chem. Lett.* **2013**, *4*, 698−703.

(7) Schmidt-Mende, L.; Bach, U.; Humphry-Baker, R.; Horiuchi, T.; Miura, H.; Ito, S.; Uchida, S.; Grätzel, M. Organic Dye for Highly Efficient Solid-State Dye-Sensitized Solar Cells. *Adv. Mater.* **2005**, *17*, 813−815.

(8) Longhi, E.; Bossi, A.; Di Carlo, G.; Maiorana, S.; De Angelis, F.; Salvatori, P.; Petrozza, A.; Binda, M.; Roiati, V.; Romana, P. M.; et al. Metal-Free Benzodithiophene-Containing Organic Dyes for Dye-Sensitized Solar Cells. *Eur. J. Org. Chem.* **2013**, *2013*, 84−94.

(9) Edvinsson, T.; Li, C.; Pschirer, N.; Schöneboom, J.; Eickemeyer, F.; Sens, R.; Boschloo, G.; Herrmann, A.; Müllen, K.; Hagfeldt, A. Intramolecular Charge-Transfer Tuning of Perylenes: Spectroscopic Features and Performance in Dye-Sensitized Solar Cells. *J. Phys. Chem. C* **2007**, *111*, 15137−15140.

(10) Cappel, U. B.; Karlsson, M. H.; Pschirer, N. G.; Eickemeyer, F.; Schöneboom, J.; Erk, P.; Boschloo, G.; Hagfeldt, A. A Broadly Absorbing Perylene Dye for Solid-State Dye-Sensitized Solar Cells. *J. Phys. Chem. C* **2009**, *113*, 14595−14597.

(11) Cappel, U. B.; Smeigh, A. L.; Plogmaker, S.; Johansson, E. M. J.; Rensmo, H.; Hammarström, L.; Hagfeldt, A.; Boschloo, G. Characterization of the Interface Properties and Processes in Solid State Dye-Sensitized Solar Cells Employing a Perylene Sensitizer. *J. Phys. Chem. C* **2011**, *115*, 4345−4358.

(12) Koops, S. E.; O'Regan, B. C.; Barnes, P. R. F.; Durrant, J. R. Parameters Influencing the Efficiency of Electron Injection in Dye-Sensitized Solar Cells. *J. Am. Chem. Soc.* **2009**, *131*, 4808−4818.

(13) Abrusci, A.; Kumar, R. S.; Al-Hashimi, M.; Heeney, M.; Petrozza, A.; Snaith, H. J. Influence of Ion Induced Local Coulomb Field and Polarity on Charge Generation and Efficiency in Poly(3-Hexylthiophene)-Based Solid-State Dye-Sensitized Solar Cells. *Adv. Funct. Mater.* **2011**, *21*, 2571−2579.

(14) Petrozza, A.; Laquai, F.; Howard, I. A.; Kim, J.-S.; Friend, R. H. Dielectric Switching of the Nature of Excited Singlet State in a Donor-Acceptor-Type Polyfluorene Copolymer. *Phys. Rev. B* **2010**, *81*, 205421.

(15) Hodgkiss, J. M.; Tu, G.; Albert-Seifried, S.; Huck, W. T. S.; Friend, R. H. Ion-Induced Formation of Charge-Transfer States in Conjugated Polyelectrolytes. *J. Am. Chem. Soc.* **2009**, *131*, 8913−8921.

(16) Cappel, U. B.; Feldt, S. M.; Schöneboom, J.; Hagfeldt, A.; Boschloo, G. The Influence of Local Electric Fields on Photoinduced Absorption in Dye-Sensitized Solar Cells. *J. Am. Chem. Soc.* **2010**, *132*, 9096−9101.

(17) Tiwana, P.; Docampo, P.; Johnston, M. B.; Snaith, H. J.; Herz, L. M. Electron Mobility and Injection Dynamics in Mesoporous ZnO, SnO_2, and TiO_2 Films Used in Dye-Sensitized Solar Cells. *ACS Nano* **2011**, *4*, 5158−5166.

(18) Tiwana, P.; Parkinson, P.; Johnston, M. B.; Snaith, H. J.; Herz, L. M. Ultrafast Terahertz Conductivity Dynamics in Mesoporous TiO_2: Sensitization and Surface Treatment in Solid-State Dye-Sensitized Solar Cells. *J. Phys. Chem. C* **2010**, *114*, 1365−1371.

(19) Docampo, P.; Tiwana, P.; Sakai, N.; Miura, H.; Herz, L. M.; Murakami, T.; Snaith, H. J. Unraveling the Function of an MgO Interlayer in Both Electrolyte and Solid-State SnO_2 Based Dye-Sensitized Solar Cells. *J. Phys. Chem. C* **2012**, *116*, 22840−22846.

(20) Snaith, H. J.; Ducati, C. SnO_2-Based Dye-Sensitized Hybrid Solar Cells Exhibiting Near Unity Absorbed Photon-to-Electron Conversion Efficiency. *Nano Lett.* **2010**, *10*, 1259−1265.

(21) Ito, S.; Chen, P.; Comte, P.; Nazeeruddin, M. K.; Liska, P.; Pechy, P.; Gratzel, M. Fabrication of Screen-Printing Pastes from TiO_2 Powders for Dye-Sensitised Solar Cells. *Prog. Photovoltaics* **2007**, *15*, 603−612.

(22) Docampo, P.; Snaith, H. J. Obviating the Requirement for Oxygen in SnO_2-Based Solid-State Dye-Sensitized Solar Cells. *Nanotechnology* **2011**, *22*, 225403.

(23) Howard, I. A.; Meister, M.; Baumeier, B.; Wonneberger, H.; Pschirer, N.; Sens, R.; Bruder, I.; Li, C.; Müllen, K.; Andrienko, D.; et al. Two Channels of Charge Generation in Perylene Monoimide Solid-State Dye-Sensitized Solar Cells. *Adv. Energy Mater.* **2014**, *4*, 1300640.